Chemical Engineering Journal 142 (2008) 209–216

Contents lists available at ScienceDirect

Chemical Engineering Journal

journal homepage: www.elsevier.com/locate/cej

Residence time distribution in continuous stirred tank electrochemical reactor

R. Saravanathamizhan [a], R. Paranthaman [a], N. Balasubramanian [a,*], C. Ahmed Basha [b]

[a] Department of Chemical Engineering, A.C. Tech. Campus, Anna University Chennai, Chennai 600025, India
[b] Department of Pollution Control, Central Electrochemical Research Institute, Karaikudi 630 006, India

ARTICLE INFO

Article history:
Received 29 October 2007
Received in revised form 21 February 2008
Accepted 26 February 2008

Keywords:
Continuous stirred tank electrochemical reactor
Residence time distribution
Three-parameter model

ABSTRACT

The aim of the present investigation is to study the electrolyte flow characteristics in a continuous stirred tank electrochemical reactor (CSTER) using residence time distribution (RTD). The flow behavior of electrolyte has been experimented using pulse tracer technique and the residence time distribution curves at various operating conditions are critically analyzed. A three-parameter model has been developed to explain the flow characteristic of electrolyte in a continuous stirred tank electrochemical reactor and the model simulations are validated with the experimental observations.

1. Introduction

Textile industries consume large amount of water for the processing and generate sizeable amount of wastewater. Textile industrial effluents have strong color due to unfixed dyes and they are biorecalcitrant due to the presence of various auxiliary chemicals such as surfactants, fixation agents, fluctuating pH and high COD. These effluents are treated by conventional treatment techniques like adsorption, biological oxidation, coagulation, etc. [1]. The conventional aerobic process, e.g., activated sludge process, cannot readily treat the effluent because most of the commercial industrial effluents are toxic to the micro organisms resulting in sludge bulking. Further, biological and chemical methods are generating solid sludge considerably, which itself requires further treatment [2]. The conventional methods of treatment have become inadequate because of their own merits and limitation when they are applied individually. In recent years, different techniques have been used, e.g., advanced oxidation technologies such as ozonation, photo oxidation, catalytic wet air oxidation and electrochemical oxidation process, etc. [3]. Among these techniques, electrochemical oxidation appears one of the most promising technologies for the treatment of wastewater. In this method, effluent is degraded without generating any secondary pollutant and this technique has certain significant advantages namely: lower temperature requirement, no sludge formation, etc. [4,5].

Various types of electrochemical reactors are used for electrochemical process. The design or selection of an appropriate electrochemical reactor for a specific purpose is important. The measurement and critical analysis of the electrolyte behavior play an important role in the effective design of an electrochemical reactor. The mathematical description of residence time distribution (RTD) is usually expressed through dispersion model or Tanks in series model [6]. A good amount of work has been reported in the literature on the performance of various types of reactors. Ferro et al. [7] studied RTD in a vessel and developed two numerical models. They reported that the measured RTD curves with numerical results successfully represent the general behavior of the fluid inside the system. de Andrade Lima and Hodouin [8] studied the flow behavior of an industrial gold leaching tank using lithium chloride tracer. The mixing pattern is modeled as two parallel flows and they reported that the tank mixing behavior is dominated by a perfectly mixed volume, corrupted by the presence of bypass and stagnant zones.

Bengoa et al. [9] developed a theoretical model for filter press type electrochemical reactor and reported residence time distribution using commercial ElectroSyn cell. The authors observed a plug flow behavior of electrolyte with both axial and lateral dispersion phenomena. Hsu et al. [10] experimented the RTD in an electrolyte solution in a micro channel that contains bundle of cylinders at low surface potential. The author reported that the shorter residence time was due to thin double layer, strong applied electric field, large applied pressure gradient, and small number of cylinders. Lidia and Marta [11] have compared $E(t)$ model conversion with experimental treatment of textile effluent reactive dye *Red Procion H-EXGL* using electrochemically generated redox mediator in a filter press cell. The authors expressed the electrolyte flow behavior using plug flow model. Polcaro et al. [12] studied the water disinfection processes in a stirred tank electrochemical reactor using boron doped diamond electrode and developed a model for $E(t)$ distribution for a pulse input considering two CSTRs in parallel.

* Corresponding author. Tel.: +91 44 22203501.
E-mail address: nbsbala@annauniv.edu (N. Balasubramanian).

1385-8947/$ – see front matter © 2008 Elsevier B.V. All rights reserved.
doi:10.1016/j.cej.2008.02.017

Nomenclature

A	surface area of the electrode (m^2)
C_{Ai}	inlet concentration
C_A	outlet concentration
$C_A^S C_B^S$	surface concentration of reactant and product at the electrode
CSTER	continuous stirred tank electrochemical reactor
COD	chemical oxygen demand
D_{a1}	Damkohler numbers
$E(t)$	exit age distribution (min^{-1})
F	Faradays law constant
i	current density ($A\,m^{-2}$)
k_{LA} and k_{LB}	mass transfer coefficients ($m\,min^{-1}$)
k_{f1} and k_{b1}	forward and reverse reactions reaction rate constants ($m\,min^{-1}$)
n	number of electrons
q	tracer quantity (mol)
Q	flow rate ($ml\,min^{-1}$)
RTD	residence time distribution
SS	stain less steel
$\bar{t}$	mean residence time (min)
V	volume of the reactor (ml)

Greek letters

α	fraction of bypass
β	fraction of active volume
$\delta(t)$	Dirac delta function (min^{-1})
γ	exchange flow ratio between active and dead zones
θ	dimensionless time
σ	interfacial area (m^{-1})

The critical review of the literature shows that extensive work has been reported on RTD studies in electrochemical reactor. However, the existing models fail to consider the dead and active regions and exchange of material between these regions. The objective of the present study is to develop a three-parameter model for residence distribution of electrolyte in a continuous stirred tank electrochemical reactor (CSTER) considering dead and active regions and exchange of material between these regions [13]. The model is evaluated at different operating conditions compared with the experimental observations.

2. Continuous stirred tank electrochemical reactor (CSTER)

Let us consider a simple electrode first-order reaction as given below

$$A + ne^- \Leftrightarrow B^+ \tag{1}$$

where 'n' refers to the number of electrons. The above reaction can be controlled either by kinetic or mass transfer. The limiting current density can be related to the mass transfer coefficient as [14]

$$i_L = nFk_mC \tag{2}$$

where k_m refers the mass transfer coefficient and C refers the bulk concentration. Let us assume the reaction takes place in a continuous stirred tank electrochemical reactor (Fig. 1) then the material balance can be written as

$$Q(C_{Ai} - C_A) = \frac{iA}{nF} \tag{3}$$

where A is surface area of the electrode and C_{Ai}, C_A are the initial and final concentrations, respectively. Eq. (3) can be written in term of residence time as

$$C_{Ai} - C_A = \frac{\sigma \bar{t} i}{nF} \tag{4}$$

where σ refers the interfacial area of the electrode. It is defined as surface area of electrode per unit volume. The electrode kinetics is assumed to follow Butler–Volmer type equations, i.e.,

$$\frac{i}{nF} = k_{f1}C_A^S - k_{b1}C_B^S \tag{5}$$

where k_{f1} and k_{b1} represent the reaction rate constants for forward and reverse reactions, respectively and C_A^S, C_B^S represent the surface concentrations.

Reaction (1) is assumed as irreversible and follows the Tafel reaction. Then the current density can be expressed in terms of the mass transport A for steady state operation as

$$\frac{i}{nF} = k_{LA}(C_A - C_A^S) \tag{6}$$

where k_{LA} represents the mass transfer coefficient of A. Eq. (5) can be written for Tafel reaction as

$$\frac{i}{nF} = k_{f1}C_A^S. \tag{7}$$

Combining Eqs. (6) and (7) the surface concentration can be eliminated resulting in surface concentration in terms of bulk concentration, i.e.,

$$\frac{i}{nF} = \frac{k_{f1}C_A}{1 + k_{f1}/k_{LA}}. \tag{8}$$

Substituting Eq. (8) in Eq. (4) and then rearranging the equation results

$$C_{Ai} - C_A = \sigma \bar{t} \frac{k_{f1}C_A}{(1 + D_{a1})} \tag{9}$$

where D_{a1} is a modified Damkohler number and can be defined as

$$D_{a1} = \frac{k_{f1}}{k_{LA}}.$$

Eq. (9) is rearranged and can be written as

$$\frac{C_A}{C_{Ai}} = \frac{1}{1 + \sigma \bar{t} k_{f1}/1 + D_{a1}}. \tag{10}$$

The above equation is reduced to

$$\frac{C_A}{C_{Ai}} = \frac{1}{(1 + P)} \tag{11}$$

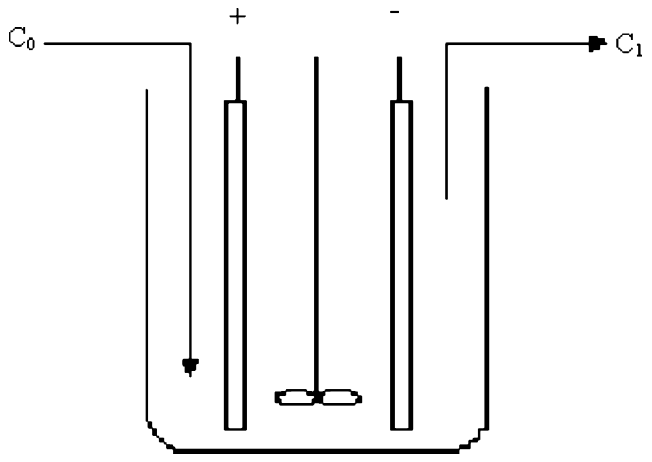

Fig. 1. Schematic representation of continuous stirred tank electrochemical reactor.

and

$$P = \frac{\sigma \bar{t} k_{f1}}{(1 + D_{a1})} \tag{12}$$

where $\bar{t}$ represents the residence time. Eq. (11) represents the conversion equation for a continuous stirred tank electrochemical reactor.

3. The RTD model

The residence time distribution of electrolyte in an electrochemical reactor can be represented by exit age distribution curve $E(t)$. At any point of time, the electrolyte spent a time between t and $(t + dt)$ in the reactor, represented by $E(t)dt$, i.e.,

$$\int_0^\infty E(t)dt = 1.0. \tag{13}$$

An ideal continuous stirred tank electrochemical reactor gives perfect mixing, and the outlet concentration is equal to the concentration inside the reactor. The CSTER can be operated either by galvanostatic or potentiostatic condition and the deviation is mainly due to the process dynamics. It is proposed in the present study that a typical CSTER consists of two zones namely active zone and dead zone. It is further assumed that there is a fractional exchange of electrolyte between active and dead zones. The schematic of the proposed CSTER model is given in Fig. 2.

The electrolyte flow to the reactor is divided into *Bypass flow* and *Active flow*, which is expressed mathematically as

$$Q = \alpha Q + (1 - \alpha)Q \tag{14}$$

where α is the fraction of electrolyte bypass and Q represents the volumetric flow rate. The *Active flow* can be related to flow through *active zone* and *dead zone*, i.e.,

$$Q(1 - \alpha)C_0 = Q\gamma(1 - \alpha)C_1' + Q\gamma(1 - \alpha)C_1'' \tag{15}$$

where γ represents the fraction of flow (i.e., $(1 - \alpha)Q$) between dead and active zones. The first and second terms in the right hand side of Eq. (15) represent the electrolyte flow through the dead and active zones, respectively. The reactor volume occupied by the dead zone, (*dead volume*) can be represented as

$$V_d = V(1 - \beta) \tag{16}$$

where V represents the total reactor volume and β represents fraction of active volume. The above equations represent the configuration arrangements of CSTER. It is further extended to study the exit age distribution of the electrolyte. The following equation is developed to represent exit age distribution in a CSTER

$$Q(1 - \alpha)C_1' + \alpha q\delta(t = 0) = QC_1 \tag{17}$$

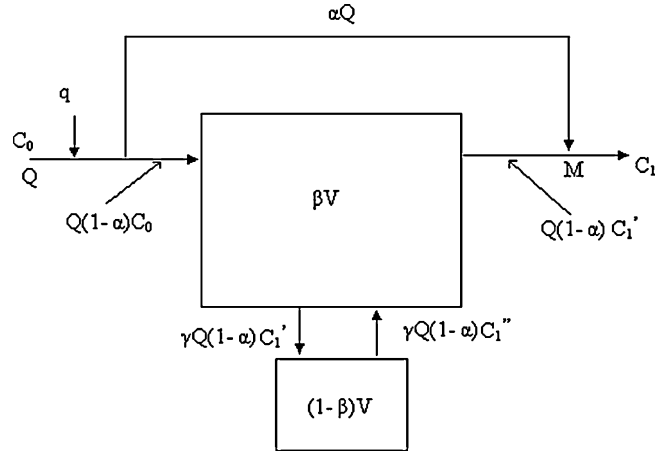

Fig. 2. Schematic representation of three-parameter model for continuous stirred tank electrochemical reactor.

where C_1 is the concentration of the tracer exit of the reactor. C_1' represents the concentration of the tracer at the exit of the active volume. Eq. (17) has been developed by taking the flow conditions outside the reactor boundary where the two streams are mixing (i.e., at the junction point M of Fig. 2). The first and second terms in the left hand side of Eq. (17) represent the flow of tracer in active zone and the bypass flow, respectively while the right hand side of Eq. (17) represents the tracer concentration at the exit of the reactor. The above equation can be used for representing pulse input by applying the condition at time $t = 0$; $q = 0$.

The material balance for active zone can be represented by the following equation

$$Q(1-\alpha)C_0 + \gamma Q(1-\alpha)C_1'' = \gamma Q(1 - \alpha)C_1' + Q(1 - \alpha)C_1' + V\beta\frac{dC_1'}{dt} \tag{18}$$

where C_1'' represents the concentration of the tracer to the active zone from the dead zone.

The first and second terms in the left hand side of Eq. (18) represent the tracer inputs to the active zone from inlet and dead zone, respectively. The first term in the right hand of Eq. (18) represents the exit from active zone to the dead zone. While the second term represents the exit from active zone to outlet. The first term in Eq. (18) is eliminated using the condition, i.e., $t = 0$; $C_0 > 0$ and $t > 0$; $C_0 = 0$.

The material balance for the dead zone can be written as

$$\gamma Q(1 - \alpha)C_1' = \gamma Q(1 - \alpha)C_1'' + (1 - \beta)V\frac{dC_1''}{dt} \tag{19}$$

The left hand side of Eq. (19) represents the input to the dead zone while the first term in the right hand side of above equation represents the output from dead zone to active zone. The above equations can be solved using Laplace transform with the following boundary condition, i.e., at time, $t = 0$; $C_1'' = 0$. The initial tracer concentration C_0 can be calculated using the following equation, i.e.,

$$C_0 = \frac{q}{V} \tag{20}$$

where the 'q' is the tracer quantity. The tracer concentration in the active zone C_1' can be related to reactor active volume as

$$C_1' = \frac{(1 - \alpha)q}{V\beta}. \tag{21}$$

The mean residence time is defined as the ratio of volume of the reactor to the volumetric flow rate.

$$\bar{t} = \frac{V}{Q} \tag{22}$$

Taking Laplace transform and rearranging Eqs. (17)–(19) yields (analytical solution of equations are given in the Appendix)

$$\frac{C_1(s)}{C_0\bar{t}} = \frac{(1 - \alpha)^2/\beta\bar{t}(s + B_1/\bar{t})}{(s - R_1/\bar{t})(s - R_2/\bar{t})} + \alpha \tag{23}$$

where B_1, B_2, B_3 represent indexes which are given as

$$B_1 = \frac{(1 - \alpha)\gamma}{1 - \beta}; B_2\frac{(1 + \gamma)(1 - \alpha)}{\gamma}; B_3 = \frac{\gamma^2(1 - \alpha)^2}{\beta(1 - \beta)} \tag{24}$$

and R_1 and R_2 are given as

$$R_1 = \frac{-1}{2}\left((B_1 + B_2) - \sqrt{((B_1 - B_2)^2 + 4B_3)}\right) \tag{25}$$

$$R_2 = \frac{-1}{2}\left((B_1 + B_2) + \sqrt{((B_1 - B_2)^2 + 4B_3)}\right). \tag{26}$$

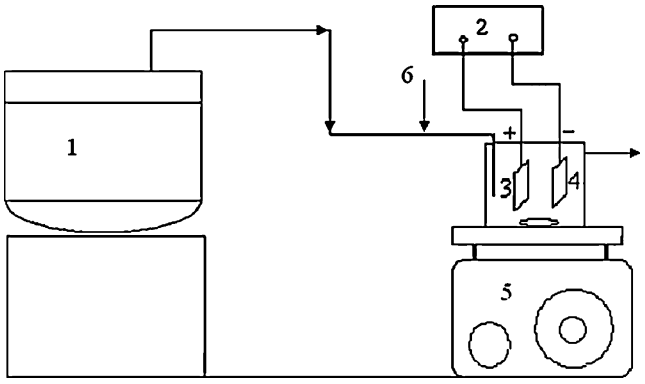

Fig. 3. Schematic representation of continuous stirred tank electrochemical reactor; (1) over head tank; (2) DC power supply; (3) anode; (4) cathode; (5) magnetic stirrer; (6) tracer injection point.

The residence time distribution function for a pulse input of tracer is obtained by taking inverse Laplace transform of Eq. (23) using a Heaviside Expansion theorem [15] as

$$E(\theta) = \frac{C_1}{C_0} = \frac{(1-\alpha)^2}{\beta(R_1 - R_2)}[(R_1 + B_1)e^{R_1 t/\bar{t}} - (R_2 + B_1)e^{R_2 t/\bar{t}}]. \quad (27)$$

Eq. (27) is used to determine the exit age distribution function of CSTER for pulse tracer input.

4. Experimental

The schematic of the experimental setup given in Fig. 3 consists of a glass beaker of 300 ml capacity with PVC lid having provision to fit a cathode and an anode. Ruthineum coated titanium and SS sheets of 6.5 cm × 5 cm were used as anode and cathode, respectively. The electrodes are fixed at 3 cm inter electrode gap. The uniform electrolyte concentration is achieved by means of magnetic stirrer. Experiments were conducted for both residence time distribution and color removal. For RTD studies, the CSTER was operated with water as electrolyte fluid. A tracer of *Acid Red 88 dye* solution was injected as pulse input and sampled periodically at the outlet of the cell. The samples were analyzed using colorimeter.

For electro oxidation, synthetic dye effluent of *Acid Red 88 dye* has been prepared at various inlet concentrations. The electrolysis was carried out under galvanostatic conditions covering a wide range of operating conditions. Samples were collected at the outlet of the reactor for the estimation of color removal at steady state conditions.

5. Results and discussion

The electrolyte behavior in a continuous stirred tank electrochemical reactor has been simulated for pulse tracer input using the model equations developed in the previous section. The simulated electrolyte flow behavior for various operating conditions is presented in Figs. 4–8. The exit age distribution $E(t)$ can be calculated from tracer output using the following equation.

$$E(t) = \frac{c(t)}{\int_0^\infty c(t)\mathrm{d}t} \quad (28)$$

where $c(t)$ represent the exit tracer concentration at time 't'. While the mean residence time can be calculated as

$$\bar{t} = \int_0^\infty tE(t)\mathrm{d}t. \quad (29)$$

The $E(\theta)$ has been calculated using Eq. (27) and converted to $E(t)$ by dividing mean residence time of the electrolyte.

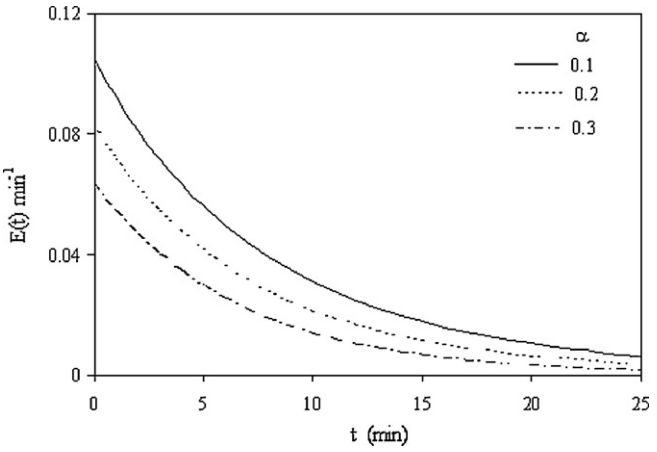

Fig. 4. Influence of reactor bypass on exit age distribution in a stirred tank electrochemical reactor; Q: 35 ml min^{-1}; β = 0.95; γ = 0.1.

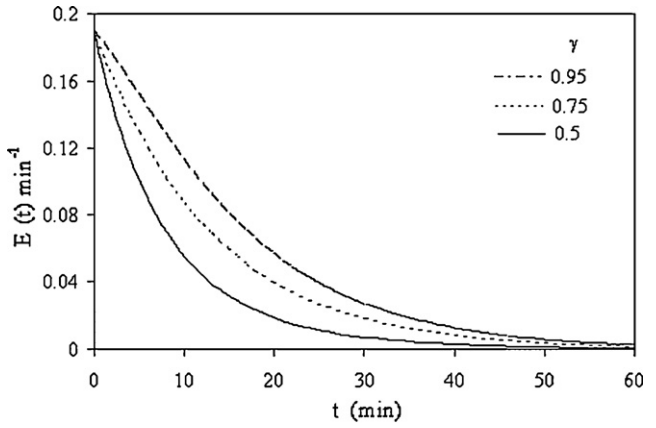

Fig. 5. Influence of exchange flow ratio on exit age distribution in a stirred tank electrochemical reactor; β = 0.5; Q: 35 ml min^{-1}; α = 0.1.

The simulated $E(t)$ with electrolysis time for various bypass ratios are given Fig. 4. It can be observed from Fig. 4 that the characteristic of age distribution curve is comparable qualitatively with conventional system. Further it is observed that the residence time distribution is increased with decrease in the reactor bypass ($Q\alpha$). It can be explained that a reduction in the reactor bypass increases the flow ($Q(1-\alpha)$) in the active zone in turn increases the electrolyte residence time.

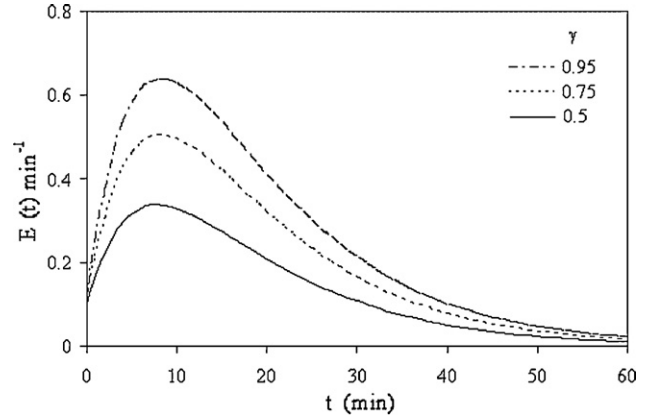

Fig. 6. Influence of exchange flow ratio on exit age distribution in a stirred tank electrochemical reactor; β = 0.95; Q: 35 ml min^{-1}; α = 0.1.

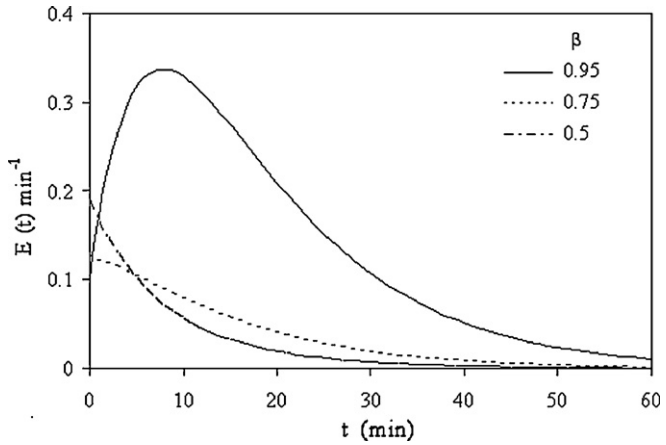

Fig. 7. The effect of active volume on exit age distribution in a stirred tank electrochemical reactor; Q: 35 ml min^{-1}; $\alpha = 0.1$; $\gamma = 0.5$.

Fig. 5 shows the effect of exchange flow ratio, 'γ' between dead and active zones on exit age distribution function. It can be ascertained from Fig. 5 that higher value of γ indicates the improved exchange of electrolyte between active and dead zones resulting increased overall effective active volume of the reactor. It can be ascertained from the Fig. 5 that the $E(t)$ for the exchange flow ratio of zero gives the age distribution of active zone leaving the entire dead zone as an ideal and not involving in the process. The Fig. 6 gives the variation of $E(t)$ with various exchange flow ratios for a given β values of 0.95. It can be ascertained from the figure that residence time distribution increases with an increase in the γ value. The age distribution curve $E(t)$ for maximum value of β and γ indicates that the entire reactor volume involves in the process.

The Fig. 7 shows the exit age distribution for various active volume fraction for a given exchange flow ratio ($\gamma = 0.5$). It can be observed from Fig. 7 that the residence time of the electrolyte is increased with increase in volume of the active zone. The maximum residence time has been observed for the active zone volume fraction of 0.95. It can be noticed from the Figs. 5 and 7 that the active volume of the reactor can be increased with increase in the exchange flow ratio (γ) and the volume of the active zone. Though the volume occupied by the dead zone ($1 - \beta$) reduces the effective volume of the reactor, the exchange flow ratio (γ) enhances the mixing between active and dead zone resulting transferring the volume occupied by the dead zone into active. The effect of flow rate of electrolyte on residence time distribution function is given in Fig. 8. The figure is drawn for three different

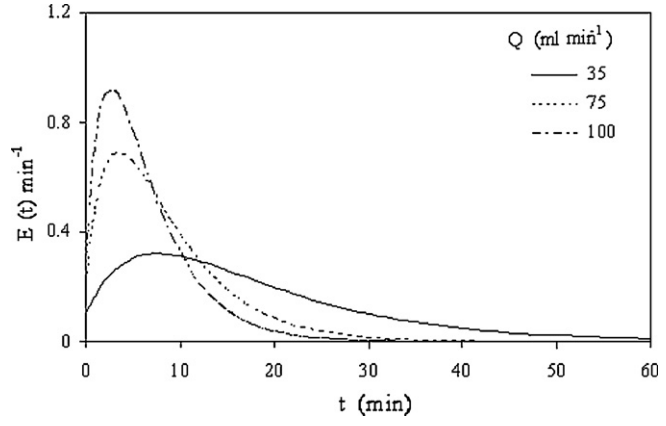

Fig. 8. The effect of electrolyte flow rate on exit age distribution in a stirred tank electrochemical reactor effect; $\alpha = 0.1$, $\beta = 0.9$, $\gamma = 0.9$.

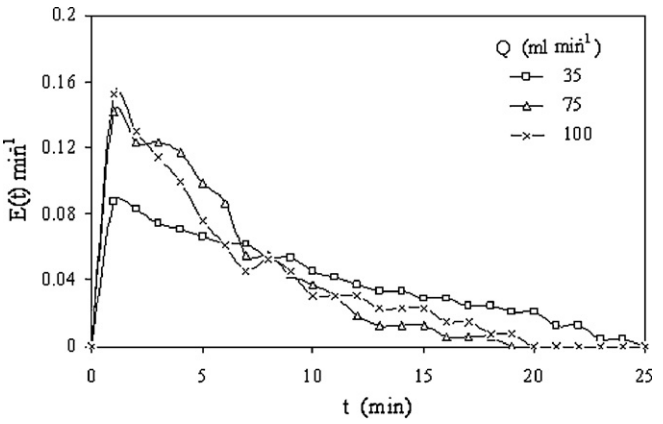

Fig. 9. The variation of experimental exit age distribution in a stirred tank electrochemical reactor.

flow rates, 35, 75 and 100 ml min^{-1} and exchange ratio of 0.9 with active volume of 90%. It can be ascertained from the Fig. 8 that an increase in the flow rate 'Q' increases the residence time distribution.

Experimental determination of residence time distribution was performed by means of tracer study. The experiments were conducted with *Acid Red 88* as tracer solution (1000 mg l^{-1}) and water as electrolyte fluid covering wide range in operating conditions. The observed results are presented in Fig. 9. It can be observed from the Fig. 9 that the residence time distribution is increased with decrease in the electrolyte flow rate. The reactor bypass value, active volume, and the exchange flow ratio have been calculated for the present experimental conditions and are presented in Table 1. As expected it can be noticed from the Table 1 that the bypass fraction and the active volume increased with the flow rate. The model predictions are compared with experimental observations and shown in Fig. 10. It can be observed from the figures that the model predictions are in good agreement with the experimental results.

Experiments were carried out for decolorization with synthetic *Acid Red 88* effluents. Experiments were conducted with constant electrolyte flow rate and samples were collected after the reactor reaching steady state and analyzed for color removal. The experimental decolorization is calculated for the different flow rate using the following relation

$$\%\text{Declorization} = \frac{C_i - C}{C_i} \times 100 \tag{30}$$

where C_i and C is the initial and final concentration of the effluent.

The residence time, the rate constant (k_{f1}) and Damkohler number (D_{a1}) were calculated from the experimental observations. These calculated values were used in the equation (11) for theoretical predictions. The experimental observation is compared with theoretical predictions and the values are given in Table 2. It can be observed from the Table 2 that the theoretical decolorization efficiency is in very good agreement with the experimental decolorization efficiency.

Table 1
The value of bypass, active volume and exchange flow ratio for the present experimental condition

	Q (ml min^{-1})		
	35	75	100
Bypass (α)	0.12	0.28	0.32
Active volume (β)	0.95	0.96	0.97
Exchange flow (γ)	0.072	0.085	0.087

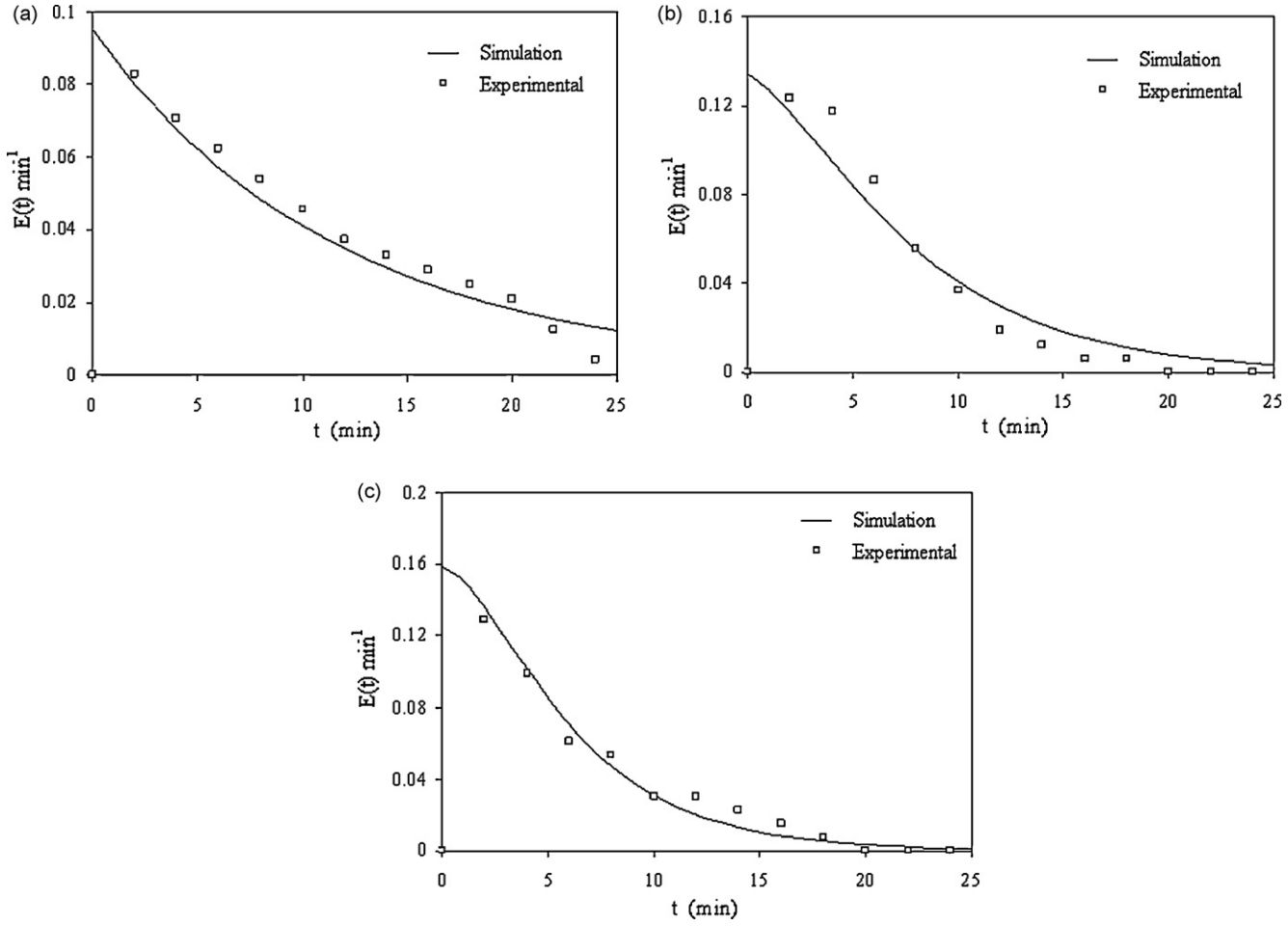

Fig. 10. Comparison of model simulations of exit age distribution with the experimental observation; (a) Q: 35 ml min^{-1}; (b) Q: 75 ml min^{-1}; (c) Q: 100 ml min^{-1}.

Table 2
Comparison of simulated percentage color removal with experimental observation: current density 10 mA cm^{-2}; initial effluent concentration: 100 mg l^{-1}; supporting electrolyte concentration: 1000 mg l^{-1}

S. no.	Q (ml min^{-1})	τ (min)	Color removal (%)	
			Theoretical	Experimental
1	35	8.59	66.14	60.50
2	75	5.33	54.79	52.23
3	100	5.23	54.32	49.04

6. Conclusion

The residence time distribution of electrolyte in a continuous stirred tank electrochemical reactor has been studied covering wide range in the operating conditions. A three-parameter model has been proposed to describe the electrolyte flow in a continuous stirred tank electrochemical reactor consisting bypass, active and dead zones with exchange flow between active and dead zones. It has been observed from the model simulations that the residence time distribution has been increased with increase in the exchange flow ratio between active and dead zones and increase in the electrolyte flow rate. Further the experiments were carried out for the effluent color removal and the values are compared with theoretically calculated value and it is observed that the values are satisfactorily matching with experimental observations.

Appendix A

Analytical solution of exit age distribution function $E(t)$ for the pulse input is given below.

The material balance is written around M in the Fig. 2

$$Q(1-\alpha)C_1' + \alpha q\delta(t=0) = QC_1 \tag{A1}$$

Material balance of the tracer in an active volume can be written as

$$\gamma Q(1-\alpha)C_1'' = Q(1-\alpha)C_1' + \gamma Q(1-\alpha)C_1' + V\beta\frac{dC_1'}{dt} \tag{A2}$$

Material balance of tracer in the dead volume can be written as

$$\gamma Q(1-\alpha)C_1' = \gamma Q(1-\alpha)C_1'' + (1-\beta)V\frac{dC_1''}{dt} \tag{A3}$$

Taking Laplace transform of the above Eqs. (A1–A3) give

$$QC_1(s) = Q(1-\alpha)C_1'(s) + \alpha q \tag{A4}$$

$$Q(1-\alpha)C_1'(s) + \gamma Q(1-\alpha)C_1'(s) + V\beta\left(sC_1'(s) - \frac{(1-\alpha)q}{V\beta}\right) = \gamma Q(1-\alpha)C_1''(s) \tag{A5}$$

$$\gamma Q(1-\alpha)C_1''(s) + (1-\beta)\left(sC_1''(s) - 0\right) = \gamma Q(1-\alpha)C_1'(s) \tag{A6}$$

Rearranging Eq. (A6)

$$C_1''(s)[\gamma Q(1-\alpha) + (1-\beta)Vs] = \gamma Q(1-\alpha)C_1'(s) \tag{A7}$$

$$C_1''(s) = \frac{C_1'(s)}{1 + (1-\beta)V/\gamma Q(1-\alpha)(s)} \quad \text{(A8)}$$

$$C_1''(s) = \frac{C_1'(s)}{1 + \bar{t}/B_1(s)} \quad \text{(A9)}$$

where

$$\bar{t} = \frac{V}{Q}$$

$$B_1 = \frac{(1-\alpha)\gamma}{(1-\beta)}.$$

Similarly Eq. (A5) is rearranged as follows

$$Q(1-\alpha)C_1'(s) + \gamma Q(1-\alpha)C_1'(s) + V\beta\left(sC_1'(s) - \frac{(1-\alpha)q}{V\beta}\right) = \gamma Q(1-\alpha)C_1''(s) \quad \text{(A10)}$$

where

$$C_1'(0) = \frac{(1-\alpha)q}{V\beta}$$

$$Q(1-\alpha)C_1'(s)+\gamma Q(1-\alpha)C_1'(s)+V\beta sC_1'(s)-(1-\alpha)q=\gamma Q(1-\alpha)C_1''(s) \quad \text{(A11)}$$

$$Q(1-\alpha)C_1'(s)+C_1'(s)[\gamma Q(1-\alpha)+V\beta s] = (1-\alpha)q + \gamma Q(1-\alpha)C_1''(s) \quad \text{(A12)}$$

$$Q(1-\alpha)C_1'(s)+C_1'(s)[\gamma Q(1-\alpha) + V\beta s]-\gamma Q(1-\alpha)C_1''(s) = (1-\alpha)q \quad \text{(A13)}$$

$$Q(1-\alpha)C_1'(s)+C_1'(s)[\gamma Q(1-\alpha)+V\beta s] = \frac{\gamma Q(1-\alpha)}{1+\bar{t}/B_1(s)}C_1''(s)+(1-\alpha)q \quad \text{(A14)}$$

$$Q(1-\alpha)C_1'(s) + C_1'(s)\left(\gamma Q(1-\alpha) + V\beta s - \frac{\gamma Q(1-\alpha)}{1+\bar{t}/B_1(s)}\right) = (1-\alpha)q \quad \text{(A15)}$$

$$C_1'(s)\left((\gamma+1)Q(1-\alpha) + V\beta s - \frac{\gamma Q(1-\alpha)}{1+\bar{t}/B_1(s)}\right) = (1-\alpha)q \quad \text{(A16)}$$

Dividing Eq. (A16) by $V\beta$ on both sides and the equation becomes,

$$C_1'(s)\left(\frac{(\gamma+1)Q(1-\alpha)}{V\beta} + s - \frac{\gamma Q(1-\alpha)}{V\beta(1+\bar{t}/B_1(s))}\right) = (1-\alpha)\frac{q}{V\beta} \quad \text{(A17)}$$

$$C_1'(s)\left(\frac{B_2}{\bar{t}} + s - \frac{\gamma(1-\alpha)}{\bar{t}\beta(1+\bar{t}/B_1(s))}\right) = \frac{(1-\alpha)C_0}{\beta} \quad \text{(A18)}$$

where

$$C_0 = \frac{q}{V}$$

$$B_2 = \frac{(1+\gamma)(1-\alpha)}{\gamma}$$

$$C_1'(s)\left(\left(s+\frac{B_2}{\bar{t}}\right) - \frac{\gamma(1-\alpha)}{\bar{t}\beta(B_1/\bar{t}+s)\bar{t}/B_1}\right) = \frac{(1-\alpha)C_0}{\beta} \quad \text{(A19)}$$

$$C_1'(s)\left(\left(s+\frac{B_2}{\bar{t}}\right) - \frac{\gamma(1-\alpha)}{(B_1/\bar{t}+s)\beta\bar{t}^2/B_1}\right) = \frac{(1-\alpha)C_0}{\beta} \quad \text{(A20)}$$

$$C_1'(s)\left[\frac{(s+B_2/\bar{t})(s+B_1/\bar{t}) - \gamma(1-\alpha)B_1/\beta\bar{t}^2}{(s+B_1/\bar{t})}\right] = \frac{(1-\alpha)C_0}{\beta} \quad \text{(A21)}$$

$$C_1'(s) = \left[\frac{((1-\alpha)C_0/\beta)(s+B_1/\bar{t})}{(s+B_2/\bar{t})(s+B_1/\bar{t}) - \gamma(1-\alpha)B_1/\beta\bar{t}^2}\right] \quad \text{(A22)}$$

$$C_1'(s) = \left[\frac{(1-\alpha)C_0/\beta(s+B_1/\bar{t})}{(s+B_2/\bar{t})(s+B_1/\bar{t}) - \gamma^2(1-\alpha)^2/(1-\beta)\beta\bar{t}^2}\right]. \quad \text{(A23)}$$

Substitute the value of (A23) in Eq. (A1)

$$QC_1(s)=Q(1-\alpha)\left[\frac{(1-\alpha)C_0/\beta(s+B_1/\bar{t})}{(s+B_2/\bar{t})(s+B_1/\bar{t}) - \gamma^2(1-\alpha)/(1-\beta)\beta\bar{t}^2}\right] + \alpha q \quad \text{(A24)}$$

Eq. (A24) is divided by V

$$\frac{QC_1(s)}{V}=\frac{Q(1-\alpha)}{V}\left[\frac{(1-\alpha)C_0/\beta(s+B_1/\bar{t})}{(s+B_2/\bar{t})(s+B_1/\bar{t})-\gamma^2(1-\alpha)/(1-\beta)\beta\bar{t}^2}\right] + \frac{\alpha q}{V} \quad \text{(A25)}$$

$$\frac{C_1(s)}{\bar{t}} = \frac{(1-\alpha)}{\bar{t}}\left[\frac{(1-\alpha)C_0/\beta(s+B_1/\bar{t})}{(s+B_2/\bar{t})(s+B_1/\bar{t})-\gamma^2(1-\alpha)/(1-\beta)\beta\bar{t}^2}\right] + \alpha C_0 \quad \text{(A26)}$$

where

$$C_0 = \frac{q}{V}$$

The denominator of Eq. (A26) is written as

$$\left(s+\frac{B_2}{\bar{t}}\right)\left(s+\frac{B_1}{\bar{t}}\right) - \frac{B_3}{\bar{t}^2} = 0 \quad \text{(A27)}$$

where

$$B_3 = \frac{\gamma^2(1-\alpha)^2}{\beta(1-\beta)}$$

Solving Eq. (A27) and the roots of the equation become,

$$R_1 = \frac{-1}{2}\left((B_1+B_2) - \sqrt{((B_1-B_2)^2+4B_3)}\right) \quad \text{(A28)}$$

$$R_2 = \frac{-1}{2}\left((B_1+B_2) + \sqrt{((B_1-B_2)^2+4B_3)}\right) \quad \text{(A29)}$$

$$\frac{C_1(s)}{C_0\bar{t}} = \frac{(1-\alpha)^2\beta\bar{t}(s+B_1/\bar{t})}{(s-R_1/\bar{t})/(s-R_2/\bar{t})} + \alpha \quad \text{(A30)}$$

$$\frac{C_1(s)}{C_0\bar{t}} = \frac{(1-\alpha)^2/\beta\bar{t}(s+B_1/\bar{t}) + \alpha(s-R_1/\bar{t})(s-R_2/\bar{t})}{(s-R_1/\bar{t})(s-R_2/\bar{t})} \quad \text{(A31)}$$

$$\frac{C_1(s)}{C_0} = \frac{(1-\alpha)^2(s+B_1/\bar{t}) + \bar{t}\beta\alpha(s-R_1/\bar{t})(s-R_2/\bar{t})}{(s-R_1/\bar{t})(s-R_2/\bar{t})\beta} \quad \text{(A32)}$$

$$\frac{C_1(s)}{C_0} = \frac{1}{\beta}\left[\frac{e^{R_1t/\bar{t}}(1-\alpha)^2(R_1/\bar{t}+B_1/\bar{t})}{(R_1/\bar{t}-R_2/\bar{t})} + \frac{e^{R_2t/\bar{t}}(1-\alpha)^2(R_2/\bar{t}+B_1/\bar{t})}{(R_2/\bar{t}-R_1/\bar{t})}\right] \quad \text{(A33)}$$

$$\frac{\beta C_1(s)}{C_0} = \frac{\bar{t}(1-\alpha)^2}{\bar{t}(R_1-R_2)}[(R_1+B_1)e^{R_1t/\bar{t}} - (R_2+B_1)e^{R_2t/\bar{t}}] \quad \text{(A34)}$$

$$\frac{C_1(t)}{C_0} = \frac{(1-\alpha)^2}{\beta(R_1-R_2)}[(R_1+B_1)e^{R_1t/\bar{t}} - (R_2+B_1)e^{R_2t/\bar{t}}] \quad \text{(A35)}$$

$$E(\theta) = \frac{C_1}{C_0} = \frac{(1-\alpha)^2}{\beta(R_1 - R_2)}[(R_1 + B_1)e^{R_1 t/\bar{t}} - (R_2 + B_1)e^{R_2 t/\bar{t}}] \qquad \text{(A36)}$$

References

[1] J. Naumczyk, L. Szpyrkowicz, F. Zilio, Grandi electrochemical treatment of textile wastewater, Water Sci. Technol. 11 (1996) 17–24.
[2] E. Razo-Flores, M. Luijten, B. Donlon, G. Lettinga, J. Field, Biodegradation of selected azo dyes under methanogenic conditions, Water. Sci. Tech. 36 (1997) 65–73.
[3] S.H. Lin, F.C. Peng, Treatment of textile wastewater by electrochemical methods, Water Res. 2 (1994) 277–282.
[4] F.C. Walsh, Electro chemical technology for environmental treatment and clean energy conversion, Pure Appl. Chem. 73 (2001) 1819–1837.
[5] T. Robinson, G. McMullan, R. Marchant, P. Nigam, Remediation of dyes in textile effluent: a critical review on current treatment technologies with a proposed alternative, Biores. Technol. 77 (2001) 247–255.
[6] A.D. Martin, Interpretation of residence time distribution data, Chem. Eng. Sci. 55 (2000) 5907–5917.
[7] S.P. Ferro, R.J. Principe, M.B. Goldschmit, A new approach to the analysis of vessel residence time distribution curves, Metall. Mater. Trans. B 32B (2001) 1185–1193.
[8] L.R.P. de Andrade Lima, D. Hodouin, Residence time distribution of an industrial mechanically agitated cyanidation tank, Minerals Engineering. 18 (2005) 613–621.
[9] C. Bengoa, A. Montillet, A. Legentilhomme, J. Legrand, Flow visualization and modelling of a filter-press type electrochemical reactor, J. Appl. Electrochem. 27 (1997) 1313–1322.
[10] J.-P. Hsu, C.-C. Ting, D.-J. Lee, S. Tseng, C.-J. Chen, A. Su, Residence time distribution for electrokinetic flow through a microchannel comprising a bundle of cylinders, J. Colloid Interface Sci. 307 (2007) 265–271.
[11] S. Lidia, R. Marta, Scale-up of an electrochemical reactor for treatment of industrial wastewater with an electrochemically generated redox mediator, J. Appl. Electrochem. 36 (2006) 1151–1156.
[12] A.M. Polcaro, A. Vacca, M. Mascia, S. Palmas, R. Pompei, S. Laconi, Characterization of a stirred tank electrochemical cell for water disinfection processes, Electrochim. Acta 52 (2007) 2595–2602.
[13] J. Raghuraman, Y.B.G. Varma, A model for residence time distribution in multistage systems with cross-flow between active and dead regions, Chem. Eng. Sci. 28 (1973) 585–591.
[14] K. Scott, Electrochemical Reaction Engineering, Academic Press, London, 1991.
[15] S.H. Mickley, T.K. Sherwood, C.E. Reed, Applied Mathematics in Chemical Engineering, McGraw-Hill, New York, 1957.